

Fast and Reliable Gravitational Waveform Model for Binary Neutron Star Coalescences

1st TEONGRAV workshop on the Theory of GW Sources

Adrian G. Abac^{1,2}

with Tim Dietrich^{1,2}, Alessandra Buonanno¹, Jan Steinhoff¹, Maximiliano Ujevic³

¹Max Planck Institute for Gravitational Physics (Albert Einstein Institute, AEI), Potsdam, Germany

²Institut für Physik and Astronomie, Universität Potsdam, Germany

³Centro de Ciências Naturais e Humanas, Universidade Federal do ABC, São Paulo, Brazil

19 September 2024
based on PRD 109 (2024) 2, 024062

► arXiv:2311.07456 [gr-qc]

Brief Recap of Existing BNS Models

Consider a frequency-domain gravitational waveform

$$h(f) = A(f)e^{-i\psi(f)}; \quad \psi(f) = \psi_0(f) + \psi_{\text{SO}}(f) + \psi_{\text{SS}}(f) + \psi_{\text{S}^3}(f) + \psi_T(f) + \dots \quad (1)$$



Tidal effects play a role in the coalescence of binary neutron stars.

1. Models geared toward describing BNS systems typically start with the analytical PN formalism
2. Current analytical knowledge for tidal effects ψ_T enter at 5PN and known up to 7.5 PN order
→ only accurate for low v , large r → often recast into the effective-one-body (EOB) formalism, including SEOBNRv4T and TEOBResumS
3. Phenomenological Models^a also exist, many directly calibrating to NR simulations, e.g. NRTidal

^aKawaguchi+ (2018). arXiv:1802.06518; Dietrich+ (2018). arXiv:1706.02969v2; Dietrich+ (2019). arXiv:1905.06011, Abac+ (2023). arXiv:2311.07456v2, Williams+ (2024). arXiv:2407.08538

NRTidalv3 at a Glance

Closed-form, modular, and efficient expression describing the (2,2)-mode tidal phase contribution of binary neutron star mergers¹

Incorporates a larger set of NR waveforms, with a wide range of EoSs, non-unity mass ratios, and dynamical tides², and is constrained with the 7.5PN expression of the tidal phase³, applicable up to merger. The frequency-domain tidal phase representation are ($\hat{\omega} = M\omega$; $x = (\hat{\omega}/2)^{2/3}$; $\bar{\kappa}_{A,B} \propto \Lambda_{A,B}$):

$$\psi_T^{\text{NRT3}} = -\bar{\kappa}_A(\hat{\omega}) \bar{c}_{\text{Newt}}^A x^{5/2} \bar{P}_{\text{NRT3}}^A(x) + [A \leftrightarrow B], \quad (2)$$

c.f. NRTidalv2:

$$\psi_T^{\text{NRT2}} = -\kappa_{\text{eff}}^T \bar{c}_{\text{Newt}}^A x^{5/2} \bar{P}_{\text{NRT2}}(x); \quad \kappa_{\text{eff}}^T = (3/16)\tilde{\Lambda}. \quad (3)$$

Reviewed and implemented in LALSuite: NRTidalv3 is almost as efficient if not more efficient than NRTidalv2.

¹Dietrich+ (2018). arXiv:1706.02969v2; Dietrich+ (2019). arXiv:1905.06011, Abac+ (2023). arXiv:2311.07456v2

²Steinhoff+ (2021). arXiv:2103.06100v2

³Henry+ (2022), arXiv:2005.13367

Recipe for NRTidalv3

$$\psi_T^{\text{NRT3}} = -\bar{\kappa}_A(\hat{\omega}) \bar{c}_{\text{Newt}}^A x^{5/2} \bar{P}_{\text{NRT3}}^A(x) + [A \leftrightarrow B]. \quad (4)$$

Frequency-Domain effective enhancement factor for the Love number:

$$\bar{k}_2^{\text{eff}}(\hat{\omega}) = 1 + \frac{s_1 - 1}{\exp[-s_2(\hat{\omega} - s_3)] + 1} - \frac{s_1 - 1}{\exp(s_2 s_3) + 1} - \frac{s_2(s_1 - 1)}{[\exp(s_2 s_3) + 1]^2} \hat{\omega}. \quad (5)$$

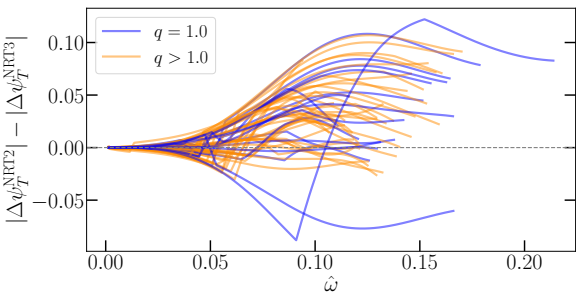
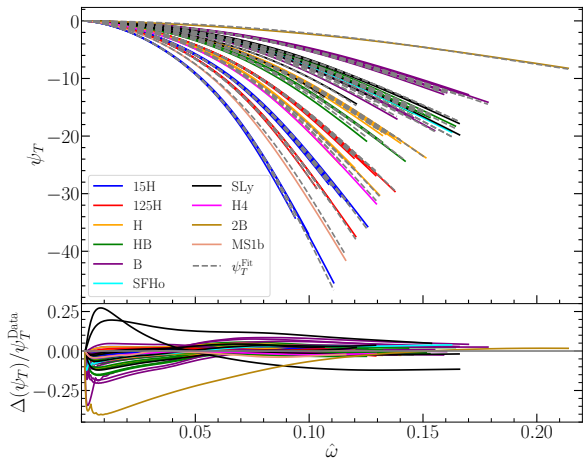
Then $\bar{\kappa}_{A,B}(\hat{\omega}) \rightarrow \kappa_{A,B} \bar{k}_2^{\text{eff}}(\hat{\omega})$. We also use the ansatz

$$\bar{P}_{\text{NRT3}}^A(x) = \frac{1 + \bar{n}_1^A x + \bar{n}_{3/2}^A x^{3/2} + \bar{n}_2^A x^2 + \bar{n}_{5/2}^A x^{5/2} + \bar{n}_3^A x^3}{1 + \bar{d}_1^A x + \bar{d}_{3/2}^A x^{3/2}}, \quad (6)$$

where $[n_{5/2}^{A,B}, n_3^{A,B}, d_1^{A,B}]$ are calibrated to EOB-NR hybrids, and the rest to the 7.5PN expression

Fits in Frequency-Domain with 55 EOB-NR Hybrids

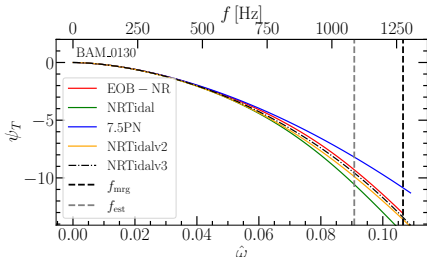
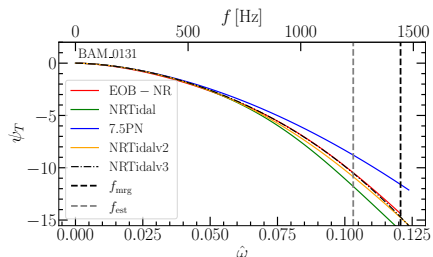
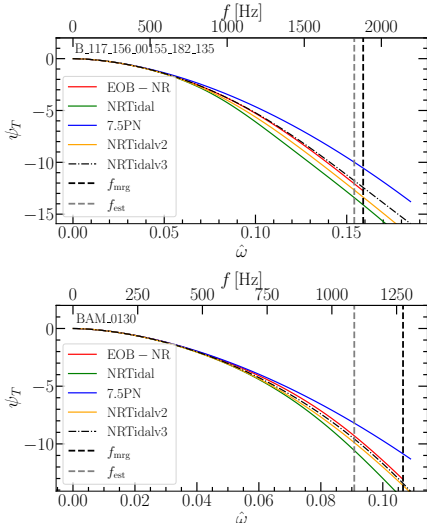
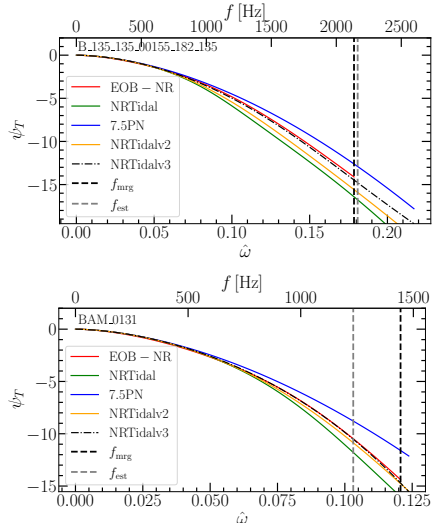
Calibration set: 55 BNS NR waveforms from SACRA and CoRe (BAM) with $\Lambda_{A,B} \in [43, 4361]$ and $q \in [1.0, 2.0]$



Fits in the Frequency-Domain for various EoS and Error Comparisons

Fits in Frequency-Domain

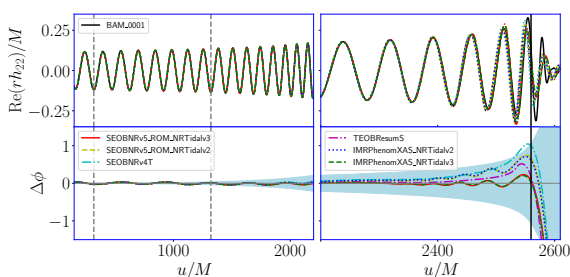
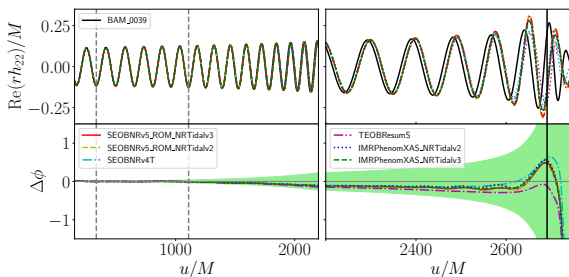
$$q = [1.0, 1.33, 1.75, 2.0]$$



Time Domain Dephasing Comparisons with NR simulations

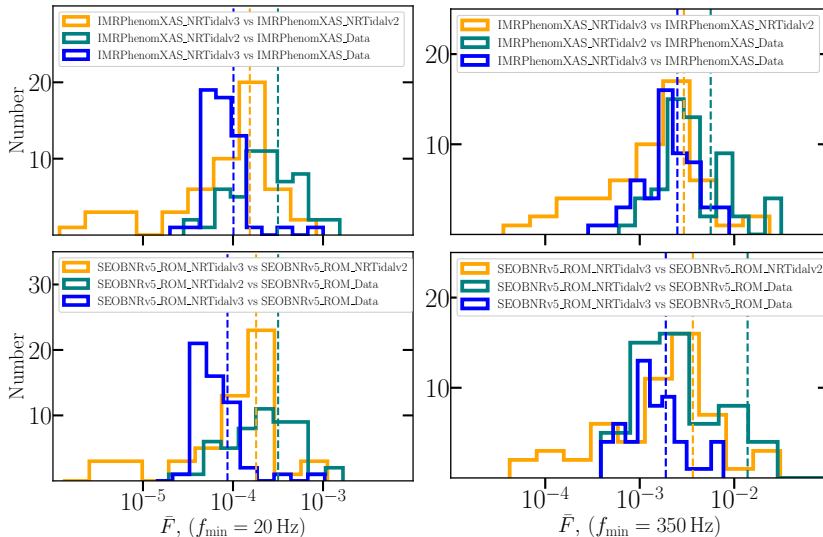
Can be employed for $M_{A,B} = [0.5, 3.0]M_\odot$, $\Lambda_{A,B} = [0, 25000]$, and $|\chi_{A,B}| \leq 0.7$

8 BAM waveforms; 2 SACRA waveforms; 2 SpEC waveforms



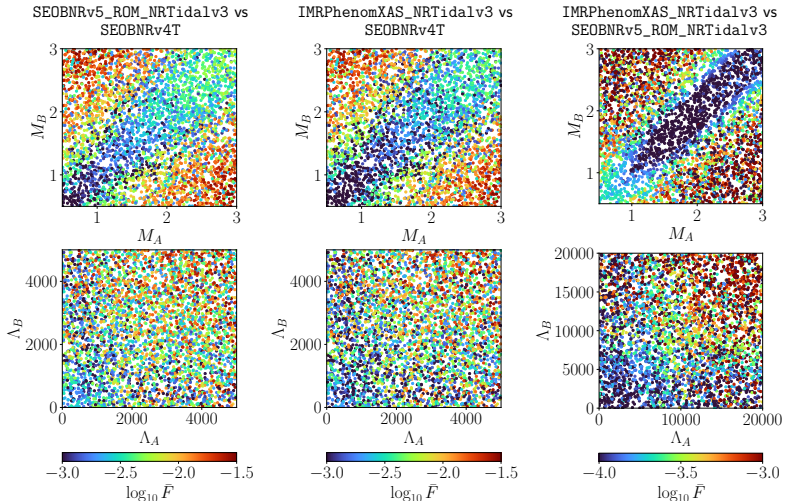
Frequency-Domain Comparisons with NR

with respect to BBH model + EOB-NR Hybrid Tidal Data



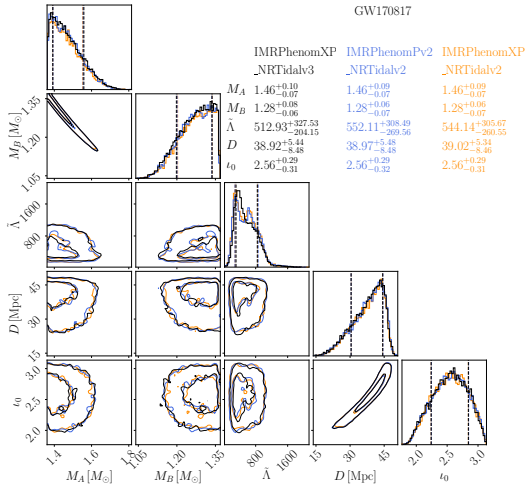
Mismatch Comparisons: Non-Spinning Case

4000 random configurations: $M_{A,B} \in [0.5, 3.0]$

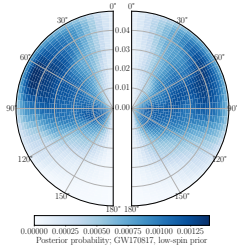


Parameter Estimation: GW170817, low-spin prior

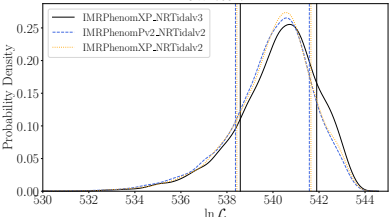
Following Bayes' theorem; speed improvements with multibanding; 30 min. for aligned spins, 60 min. for precessing spins



GW170817

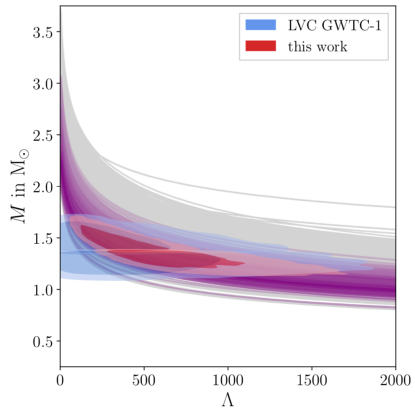


GW170817

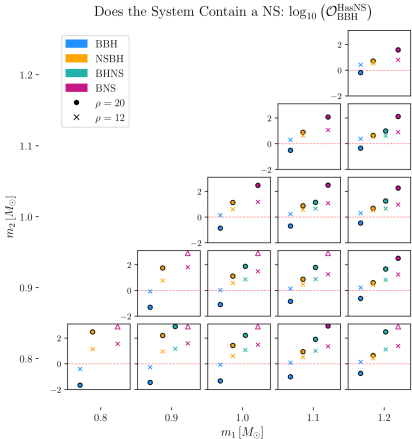


Consistent results with previous LVK analyses (the same with GW190425 and high-spin priors)

Some Applications of NRTidalv3



$M - \Lambda$ curves color-coded according to the posterior likelihood based on inference with GW170817
Koehn+ (2024). arXiv:2402.04172



Odds-ratios for different binary systems at various mass ratios
Golomb+ (2024). arXiv:2403.07697

Takeaways and Outlook

NRTidalv3 improves upon previous versions by including dynamical tidal effects, larger NR set for calibration with high-mass ratios across various EOSs.

NRTidalv3 is as efficient, if not more efficient than NRTidalv2 counterparts, despite more physics included and the more complicated form.

Available in LALSuite, and can be employed for $M_{A,B} \in [0.5, 3.0]M_\odot$, $|\chi_{A,B}| \leq 0.7$, and $\Lambda_{A,B} \in [0, 25000]$

Consistent with previous LVK PE analyses with slightly tighter constraint on $\tilde{\Lambda}$, also slight (but statistically insignificant) preference for IMRPhenomXP_NRTidalv3 than IMRPhenomPv2_NRTidalv2 and IMRPhenomXP_NRTidalv2

Has been applied in constraining the EOS of supranuclear dense matter

Potential extensions include higher-mode waveforms and calibration to future NSBH systems